Fast pyrolysis of agroindustrial wastes blends: hydrocarbon production enhancement

A. Alcazar-Ruiz, F. Dorado, L. Sanchez- Silva*

Department of Chemical Engineering, University of Castilla –La Mancha,

Avda. Camilo José Cela 12, 13071 Ciudad Real, Spain

*Corresponding author phone: +34 926 29 53 00 ext. 6307; fax: +34 926 29 52 56;

e-mail: marialuz.sanchez@uclm.es

Abstract

Fast pyrolysis of waste from agroindustry may be an alternative choice for sustainable use of enhanced biofuels. Plastics are one option for improving the hydrogen to carbon efficiency ratio (H/C_{eff}) of biomass feedstock. Waste from agroindustry in blends with biomass could modify the reaction mechanism for removing oxygen by substituting decarbonylation and decarboxylation with dehydration. Firstly, fast pyrolysis was performed to find the optimal mass blending ratio for olive pomace (OP) and agroindustrial polymers (polyethylene (PE), polystyrenes (PS) and polyvinyl chloride (PVC)) according to hydrocarbon production. Experimental results for the 1.5:1 OP/PE, 1:1.5 OP/PS and 1:1.5 OP/PVC mass blending ratios at 500 ºC, showed synergistic enhancement of hydrocarbon yields. Alkenes yield were enhanced for 1.5:1 OP/PE, where the light hydrocarbons fraction (C_6-C_{10}) first increased and then decreased with temperature, reaching a maximum at 650 ºC. For 1:1.5 OP/PS and 1:1.5 OP/PVC, it was improved the aromatic compounds formation, being 500 ºC and 650 ºC the optimal reaction temperature for the former and the later, respectively. Benzene, toluene and xylene were in large quantities obtained for PS and PVC blends with OP. Additionally, the synergistic effect on pyrolysis of the blends did not show any clear trend for pyrolytic gas emissions. In general, as reaction temperature increased, CO and CO_2 emissions fell and CH_4 was enhanced. Finally, olefin and aromatic yields were promoted for blends with a higher H/C_{eff}.

Keywords: Fast pyrolysis; Olive pomace; Agroindustrial polymers; Hydrocarbon production; Synergistic effect; H/C_{eff}

1. Introduction

Growing concerns with the imminent depletion of fossil fuels and their adverse environmental effects have led to a focus on using renewable lignocellulosic biomass as an alternative energy resource. Olive oil production and related industries are of great importance in terms of wealth, health and tradition in the Mediterranean area [1]. However, this industry generates olive pomace in high amounts as waste from agroindustry and there have been moves to valorise this. Dried olive pomace contains a high amount of organic matter, water-soluble fats, proteins, water-soluble carbohydrates and water-soluble phenolic substances [2]. Therefore, this olive waste could be used as a sustainable biomass feedstock for creating valuable products, thereby reducing the impact the olive oil industry has. In addition, the hydrogen to carbon effective (H/C_{eff}) ratio plays a significant role in the conversion efficiency of biomass into valuable products. Thus, it is logical to add high hydrogen yield co-reactants to lignocellulosic biomass, hence modifying the reaction mechanism of oxygen removal by substituting decarbonylation and decarboxylation with dehydration, which enhances the hydrogen deficient biomass [3].

Plastic waste is seen as one option for improving the hydrogen to carbon efficiency of sustainable biomass feedstock due to its hydrogen-rich nature [4]. Furthermore, plastic materials have similar properties to those in fossil fuels in terms of heating value and lack of oxygenated compounds. Currently, the most widespread plastics used are polyethylene (PE), polypropylene (PP), polystyrenes (PS), polyvinyl chloride (PVC) and polyethylene terephthalate (PET). For over 50 years, plastics have been made for improving our standard of living [5]. Consequently, annual global consumption of plastics has surpassed 300 million tonnes [6]. Due to its high consumption, managing this waste material is of great social and environmental concern. At present, recycling these residues is a growth

area. In Europe, only 32.5% of plastic waste generated in 2019 was recycled, while the rest was landfilled or used in energy recovery processes [7]. To be specific, plastic waste from agroindustry represents 2% of total plastic waste generated [8].

To reduce such wastes, different thermochemical methods such as pyrolysis have been promoted as one solution. Pyrolysis of plastic waste in an inert atmosphere is regarded as one of the most viable recycling methods for obtaining valuable products [9]. Three pyrolysis processes can be differentiated depending on operating conditions, each of which is aimed at producing desirable products. Fast pyrolysis leads to high bio-oil production (approximately 75 wt.%) and occurs at high heating rates, moderate temperatures and short residence time [4,10,11]. Operating conditions for fast pyrolysis can easily be adjusted to maximise bio-oil production and the quality of the products obtained [12]. Furthermore, in this process plastic could act as a source of hydrogen atoms, producing hydrocarbons with a similar composition found in conventional gasoline [13]. Therefore, co-pyrolysis could be a promising solution since it can easily process waste from biomass and plastics, tackling different challenges simultaneously and converting them into high value fuels or chemicals [14]. In co-pyrolysis, high oil yields are achieved at temperatures from 400 to 600 ºC, and the optimum temperature for maximum oil yield depends on the proportions and characteristics of the feedstock [4]. Moreover, co-pyrolysis of woody biomass and plastic waste produces high yields in terms of forming hydrocarbons while oxygenated compounds such as ketones, aldehydes and acids are suppressed [15]. However, any improvements in the yield and quality of bio-oil is attributed to various synergistic interactions between the feedstocks [4,16,17].

Research data on biomass and plastic pyrolysis usually focus on bio-oil properties and yield, rather than the synergistic mechanism. The synergy effect between biomass and polymers in co-pyrolysis is the main factor behind bio-oil quality and any improved

quantity [3]. It usually occurs when the combined effects of the components are greater than the sum of their individual ones. Ephraim et al. analysed the synergistic effect and product yield for various plastic materials and saw that product composition depends on feedstock [18]. Li et al. studied the maximum content of hydrocarbons from catalytic fast co-pyrolysis of rice husk and plastic films waste from greenhouses, at a maximum temperature of 600 °C with a mass ratio of 1:1.5 [19]. Mixtures of biomass sawdust and waste polyolefins from packaging for dairy products revealed maximum hydrocarbon production were achieved with 75% of PS blends [13]. In general, the literature has established a positive synergy between biomass and plastics, which results in enhanced aromatic hydrocarbon yields due to the higher calorific values and H/C_{eff} ratio in plastics compared to biomass [20,21]. Nevertheless, there are no studies that focus on the synergistic enhancement of olive pomace in blends with plastic wastes in which pyrolysis product distribution is valorised.

In this study, olive pomace is co-pyrolysed with waste polymers (PE, PS and PVC) to valorise these agroindustrial subproducts and to research the influence of plastic content on bio-oil properties. Furthermore, olive pomace and the polymers mass ratio (OP/P ratio) and the effect of reaction temperature were studied to evaluate the synergies, hydrocarbon composition in bio-oils, and the hydrogen to carbon effective ratios derived from fast pyrolysis mixtures.

2. Materials and methods

2.1. Materials

Olive pomace (OP) was supplied by Aceites García de la Cruz olive oil mill (Madridejos, Castilla-La Mancha, Spain). Prior to the experiments, OP was first oven-dried for 24 h at 100 ºC and milled and sieved to a obtain an average particle size ranging from 100 to 150

120 µm. The polymers used (PE, PS and PVC) were purchased from Sigma-Aldrich, US. The
121 plastics received were ground and sieved to a particle size of under 0.1 mm.

122 2.2. Sample characterisation

123 Materials were first characterized by elemental and thermogravimetric analysis in a TGA
124 apparatus (TGA-DSC 1, Mettler Toledo). The ultimate and proximate analysis were
125 carried out according to standards UNE 15104:2011, UNE-EN ISO18123:2016, UNE 32-
126 004-84 and UNE 32-002-95, in a Thermo Fischer Scientific Flash 2000 elemental
127 analyser, equipped with a thermal conductivity detector. The proximate analysis provided
128 data on moisture, ash, volatile matter and fixed carbon content. Also, the ultimate analysis
129 was used to find the concentration of carbon, hydrogen, nitrogen, oxygen and sulphur in
130 the sample. The higher heating value (HHV) can be calculated using the ultimate analysis
131 data with the following empirical correlation (eq. 1, [22]; Table 1):

132 $$HHV\ (MJ/kg) = 0.3491 \times C + 1.1783 \times H + 0.1005 \times S - 0.1034 \times O - 0.0151 \times N -$$
133 $$0.0211 \times A \quad \text{(eq. 1)}$$

134 In which C, H, S, O and N are the weight percentages of carbon, hydrogen, sulphur,
135 oxygen and nitrogen respectively, whereas A is the weight percentage of ash.

136 In addition, metal content was determined by Inductively Coupled Plasma-Optical
137 Emission Spectrometry (ICP-OES) with Varian 720-ES equipment (which was
138 previously calibrated using standard stock solutions). The ratios of extractives,
139 hemicellulose and Klason lignin in OP were tested according to the TAPPI 204 om-97
140 and TAPPI T222 om-02 method [23,24] whose results are shown in Table 1.

141 The chemical structure of the obtained residual carbon after fast pyrolysis was
142 characterized by: Resolution Scanning Electron Microscope (HRSEM), carried out using
143 a Gemini SEM 500 High from ZEISS brand (Oberkochen, Germany); Energy Dispersive

144 X-Ray Analyses (EDX), carried out in an Oxford brand instrument at 15.00 kV
145 accelerated voltage and 127x magnifications; and finally, FTIR spectroscopy, performed
146 with a Perkin-Elmer FTIR Spectrum-two spectrophotometer provided with a Universal
147 Attenuated Total Reflectance accessory (UATR). The spectra accumulated 64 scans with
148 a range between 500 and 4000 cm^{-1} and a resolution of 8 cm^{-1}.

149 2.3.Fast co-pyrolysis experiments, conditions and procedure analysis

150 The co-pyrolysis experiments were performed with OP and PE, PS and PVC via Py-
151 GC/MS-FGA (CDS Pyroprobe 6200 pyrolyser; Agilet Technologies 7890B/5977B
152 GC/MS, and CDS Analytical Model 5500 Fixed Gas Analyser). A schema of the
153 experimental setup is presented in Fig. 1.

154 The GC/MS injector temperature was kept at 280 ºC. An Elite-35MS capillary column
155 (30 m x 0.25 µm) was used for chromatographic separation. Helium (99.999 %) was
156 selected as the carrier gas at a constant flow rate of 1 mL/min and a 1:80 split ratio. This
157 was carried out to separate and identify the chemical composition of the bio-oil. Oven
158 temperature was programmed from 40 ºC (3 min) to 280 ºC at a heating rate of 5 ºC/min.
159 The chromatograms were integrated, and relative peak areas were calculated and
160 subsequently identified using the NIST library as a reference and only those with over an
161 80% matching quality were considered. The FGA used a 1/8" packed column and thermal
162 conductivity detector to analyse the gases produced during fast pyrolysis that were not
163 easily assayed using capillary GC/MS. The absorbent trap of the pyrolyser collected the
164 organic products from pyrolysis and transferred them to the GC/MS as usual.
165 Different experiments were performed by varying the OP/P ratio (1.5:1, 1:1, 1:1.5, and
166 1:2), by keeping the total feedstock mass at 1 mg ± 0.05 mg and placing it in the middle
167 of a quartz tube (2 mm diameter and 20 mm long) with a quartz wool base. The heating

rate and the reaction time of fast pyrolysis were optimized, set at 20 ºC/ms, and 20 s [2]. Firstly, fast pyrolysis took place at 500 ºC to determine the optimum mass ratio. Subsequently, the influence of temperature on product distribution was performed at 500, 550, 600, 650, and 700 ºC. The experiments were carried out in triplicate for each sample to ensure reproducibility.

The peak area based on the Py-GC/MS and Py-FGA analysis could not show the real content in the target compounds. However, if the mass of the sample was the same in each pyrolysis experiment, the corresponding chromatographs could be compared to reveal the proportion of components in the bio-oils produced.

2.4. Effective hydrogen to carbon molar ratio (H/C_{eff})

The effective hydrogen to carbon molar ratio (H/C_{eff}) is used to describe whether a feedstock can be upgraded or processed at existing refineries [25]. This factor shows the potential the feedstock has for converting it economically to hydrocarbons, and helps estimating the overall yield of olefin and aromatics [26]. The definition of H/C_{eff} is calculated by using the number of moles of the feedstock with the following equation [16]:

$$H/C_{eff} = (H - 2O - 3N - 2S) / C \quad \text{(eq. 2)}$$

Higher H/C_{eff} ratios in the feedstock implies more efficient conversion at refineries. This ratio is also shown by many researchers to estimate how a feedstock can be economically converted to hydrocarbons using a potential catalyst. The H/C_{eff} ratio of petroleum-derived feedstocks is between 1 and 2 and that for lignocellulosic biomass is between 0 and 0.3 [27]. Therefore, pyrolysis oil from the latter feedstock may be considered to have hydrogen-deficient molecules when compared to those in the feedstock at the current petroleum refinery [25]. Therefore, to obtain pyrolysis oil with a high H/C_{eff} ratio,

192 agroindustrial plastics could be a potential hydrogen donor feedstock, to produce
193 enhanced bio-oil.

194 2.5.Synergistic evaluation

195 To obtain a comprehensive analysis of the results, theoretical values expected from each
196 experiment were calculated by considering the proportion of mixtures as an arithmetic
197 sum of the values obtained by single-feedstock fast pyrolysis, assuming there were no
198 chemical interactions between either feedstock during devolatilisation. This method may
199 be considered as one of the best approaches for analysing synergistic effects in properties
200 after any pyrolytic process, since bio-oils from lignocellulosic biomass are not miscible
201 with polyolefin oils [28].

202 **3. Results and discussion**

203 3.1. Thermal behaviour of olive pomace and agroindustrial plastics

204 Fig. 2 shows the thermogravimetric (TG) and the derivate thermogravimetric (DTG)
205 curves obtained for OP, PE, PS and PVC. The main pyrolysis stage for OP took place at
206 temperatures between 120 and 450 ºC, as seen from their DTG profile in Figure 2b. For
207 OP, the shoulders observed at around 280 and 350 ºC were attributed to hemicellulose
208 and cellulose decomposition, respectively. These peaks were followed by a tail, which
209 was ascribed to lignin decomposition, leading to char formation. However, a small peak
210 was observed for olive pomace at nearly 400 ºC, which could be attributed to lipid
211 decomposition of the olive oil [29]. One outstanding observation was that the thermal
212 stability of the biomass was lower than that for the plastics during pyrolysis. Thus, the
213 free radicals arising when the biomass degraded might have promoted decomposition of
214 plastic-derived macromolecules [3]. Moreover, thermal degradation of PE took place at
215 a higher temperature range (410-520 ºC) and was completed at 520 ºC. As seen with the

behaviour of PE, the PS sample was thermally degraded from 350 to 500 ºC. In general, thermal decomposition of most synthetic polymers (such as PE and PS) occurs by random scission and radical mechanisms: initiation, propagation and termination [30]. The carbon-to-hydrogen (C–H) bonds of primary, secondary, and tertiary carbon atoms, and carbon-to-carbon (C–C) sigma bond are the only ones that makes probability distribution in bond selection for radical formation or breakage [3]. However, in straight chain polymers, the main products formed are hydrogen gas and hydrocarbons [4]. In contrast with the thermal behaviour seen with PVC, two peaks are observed that correspond to two degradation stages. The first one occurred in the 240-410 ºC temperature range. The dominant reaction here was dehydrochloration in which HCl and other chlorinated hydrocarbons were released. The second peak occurred in the 410-540 ºC interval, in which rearrangement and cyclisation of conjugated polyene were the main reactions and the benzene derivates generated. This indicates that carbon-chloride bonds during pyrolysis has less energy than that in C-C bonds [31]. Furthermore, note that the loss in mass could have occurred earlier when PVC was in the blend, indicating that promoted pyrolysis products could have occurred at lower temperatures [26]. In conclusion, those polymers selected could provide hydrogen, which is lacking in OP, due to the range of temperatures in fast pyrolysis. Also, there may have been improvements to product distributions for the OP/P blends.

3.2. Effect of OP/P mass ratio on product distribution

To analyse the influence of adding agroindustrial polymers (PE, PS and PVC) to product distribution, different OP/P mass blending ratios were evaluated. The optimal OP/P mass ratio was selected taking into account the hydrogen to carbon effective $(H/C)_{eff}$ ratio which efficiently converted OP into elaborate biofuels. However, this data could demonstrate synergistic enhancement on hydrocarbon product distribution. Also,

241 polymers with different $(H/C)_{eff}$ ratios were selected to be studied in a mixture with OP
242 through fast pyrolysis to observe whether there was an improvement in hydrocarbon
243 production efficiency or not. It must be stressed that fast pyrolysis temperature was set at
244 500 ºC. First, raw samples of the materials under study were pyrolysed to establish their
245 product composition. The results showed significant differences in pyrolysis product
246 distribution for OP and agroindustrial polymer samples. The relative percentage of
247 hydrocarbons in OP bio-oil reached a maximum of 25%, while the remainder were the
248 oxygenates formed based on alcohol, aldehydes, acids, esters, ketones and phenols. The
249 most representative group identified in OP pyrolysis were phenolics from the thermal
250 decomposition of lignin [23]. In contrast, from pyrolysis product distribution of
251 agroindustrial polyolefins at 500 ºC, hydrocarbons were the main functional group
252 detected, and they accounted for nearly 100%. The theoretical (Theo) and experimental
253 (Exp) data for the carbon yield (%) of each functional group detected after fast pyrolysis
254 of the different OP/P mass ratios were compared to study the synergistic effects.
255 Theoretical carbon yield (CY_{th}) can be calculated as follows [29]:

256 $$CY_{th} = CY_{OP} \cdot F_{OP} + CY_{P} \cdot F_{P} \quad \text{(eq. 3)}$$

257 Where F_{OP} and F_{P} are the mass fraction of olive pomace and polyolefin used (varied PE,
258 PS and PVC), and CY_{OP} and CY_{P} are the carbon yields (%) obtained from fast pyrolysis.
259 A positive rise in carbon yield production in comparison with the theoretical value of the
260 blend could be deemed a synergistic effect in which more hydrocarbons are formed. Fig.
261 3 summarised this effect on hydrocarbon distribution for the different OP/P mass ratios
262 with the fast pyrolysis experiments performed at 500 ºC.

263 Figure 3 compares theoretical and experimental carbon yields of total hydrocarbons
264 produced from fast pyrolysis for different OP/P mass blending ratios. With PE, its product

265 distribution is mainly based on hydrocarbons, with alkanes being the most representative
266 group detected, with a yield of 64.17%. The PE composition gave rise to a greater HHV
267 of 41 MJ/kg (Table 1), similar to those in commercial fuels, such as gasoline or diesel
268 [32]. However, PE in blends with biomass feedstock was expected to reduce the oxygen
269 content at the organic phase whilst carbon yield increased, leading to a higher HHV. The
270 synergistic effect between the OP/PE mass blending ratios during fast pyrolysis has been
271 discussed. In Fig. 3a, synergy was detected on comparing theoretical and experimental
272 hydrocarbon formation for OP/PE blends. Aliphatic hydrocarbons derived from pyrolysis
273 of PE might have interacted with the oxygenate fraction present in OP through a series of
274 cracking, cyclization and isomerization reactions, thereby increasing hydrocarbon
275 diversity (alkenes and cyclic hydrocarbons) [16]. According to the results, the 1.5:1
276 OP/PE mass blending ratio produced the highest percentage of hydrocarbons. The
277 maximum percentage of hydrocarbons reaches a maximum of 89.73% at 500 ºC. The
278 hydrocarbons obtained are mostly aliphatic compounds, especially long chain olefins, and
279 they amount to 79.44% of total condensable compounds. Thus, it may be concluded that
280 mixtures of OP and PE by fast pyrolysis can modify the reaction mechanism, thereby
281 removing oxygenates by substituting decarbonylation and decarboxylation with
282 dehydration [3]. Previous studies have demonstrated the modification of reaction pathway
283 of the co-feeding of lignocellulosic biomass with hydrogen-rich feedstocks in catalytic
284 pyrolysis [33–35]. In addition, hydrogen abstraction by OP oxygenates and reactive free
285 radicals could facilitate thermal degradation of PE, which explains the synergy on
286 increasing aliphatic hydrocarbons [3].

287 Regarding Fig. 3b, from the OP/PS blends, positive synergy was observed with an
288 increase in hydrocarbon, specifically the carbon yield of aromatic compounds. Bio-oil
289 composition obtained from PS fast pyrolysis was shown to be oxygen-free. It has

290 significant hydrocarbon content which amount to 64.54% of carbon yield. In comparison
291 with PE, PS has a low aliphatic content due to its aromatic ring. Also, PS has a similar
292 HHV to commercial liquid fuels, and has the capacity to reducing oxygen increasing
293 carbon yield. Different OP/PS mass ratios were studied to observe the synergistic effect
294 in fast pyrolysis by comparing theoretical and experimental results. The aromatic yields
295 obtained are discussed between ratio blends. Moreover, the 1:1.5 OP/PS mass blend ratio
296 provided the highest percentage of hydrocarbons. The relative content of hydrocarbons
297 in this blend represented 96.23% of carbon yield at 500 ºC, in which 68.57% of the
298 condensable compounds detected were aromatics. These results were coherent with the
299 literature, in which adding PS in blends with lignocellulosic biomass enhanced the quality
300 of the bio-oil obtained, as oxygenated compounds transformed into aromatics [36–38].

301 Some special polymers, such as PVC, has attracted attention for use in co-pyrolysis. PVC
302 was selected despite its low H/C_{eff} in comparison with other polyolefins. In Fig. 3c, a
303 synergistic effect in the OP/PVC blends by fast pyrolysis at 500 ºC was assumed. Results
304 revealed hydrocarbon compounds were the main product obtained from PVC pyrolysis,
305 with aromatics being the most representative hydrocarbon with 53.43% of total carbon
306 yield. Zhou et al. researched the pyrolysis mechanism for PVC, and explained that
307 formations of aromatics can be ascribed to molecular rearrangement and cyclisation of
308 fragments of polyene [31]. PVC has low HHV, which may not help to reduce oxygen
309 content in blends with OP. Moreover, OP has a higher H/C_{eff} ratio in comparison to PVC.
310 The hydrogen content in OP could act as a hydrogen donor for PVC in fast pyrolysis. In
311 this case, water evolved from OP pyrolysis could also act as a reactive compound, thereby
312 accelerating further cracking of PVC, and hence, promoting yields of bio-oil [3].
313 Furthermore, PVC chloride atoms are unstable and easily split at higher temperatures.
314 Dehydrochlorinated and chlorinated hydrocarbons were formed at temperatures below

500 ºC. As the pyrolysis temperature was set at 500 ºC, chloride compounds were not detected in this study. Additionally, removing HCl typically includes alkali and alkaline earth metal substances as absorbents, as the inherent metals presents in the organic matrix of OP [31]. This will be discussed in more detail below. The blend with the 1:1.5 OP/PVC mass ratio produced the highest carbon yield of hydrocarbon compounds (85.23%) at 500 ºC, in which 54.04% of the components detected were aromatics.

These results demonstrated the synergy observed on comparing theoretical and experimental data. This proved to have an apparent effect on bio-oil hydrocarbon production, thus enhancing use of OP [16]. Additionally, one of the forms to evaluate the bio-oil quality is through its calorific value. Closely, this depends on carbon, hydrogen and oxygen contents, as well as the H/C_{eff} ratio. When plastics are used in the reaction, this ratio increases due to the contribution of the H atoms that the plastics provide, and consequently the O atoms decrease, thus increasing the calorific value [39]. For this reason, synergy was obtained between OP and agroindustrial polyolefins (PE, PS and PVC), where the oxygenates were reduced and hydrocarbon compounds fomented. Indeed, this effect was supported by the effective hydrogen to carbon ratio values obtained for the blends. The carbon yields of hydrocarbon compounds in bio-oil with H/C_{eff} ratios are given in Fig. 4. The convex parabolic curves in Fig. 4a and 4b demonstrate there is a synergistic effect between OP and PE or PS blends in fast pyrolysis. Alkenes production reached a maximum carbon yield for the 1.5:1 OP/PE blend ratio, in which the H/C_{eff} mixture marked 0.88. This result suggests that the 1.5:1 OP/PE ratio should mean there is enough hydrogen added to the blend to maximise hydrocarbon products. However, this small amount of PE in the blend could stabilize most of the unstable compounds in the bio-oil by hydrogenation. The unstable molecules that tend to increase coke formation include oxygenates with unsaturated bonds [27]. Conversely,

aromatic compounds reached maximum yields when OP/PS and OP/PVC blend ratios were 1:1.5, in which H/C_{eff} was 0.66 and 0.11, respectively. Remarkably, in OP/PVC mixtures aromatic production synergy was observed in the bio-oils produced, even though PVC showed a low hydrogen to carbon effective value. Despite this, PVC was characterised as hydrogen-rich and intermediate in a blend with OP during fast pyrolysis. Furthermore, oxygenated chemical bonds from the OP organic matrix could favour chain scission and breakages in long-chain organic matter in polyolefins [3]. The convex curves shown demonstrate synergy in the OP/P blends. Thus, this may indicate that thermochemical processes efficiently convert more undefined oxygenates into hydrocarbons when producing bio-oil from these blends. The best options for OP/P mass blending ratios were 1.5:1 OP/PE, 1:1.5 OP/PS and 1:1 OP/PVC. These were the optimal proportion of polyolefins and OP feedstock for enhancing olefin and aromatic compounds production yields.

3.3. Influence of reaction temperature on fast pyrolysis products for the OP/P mass ratios selected

To study the influence of fast pyrolysis temperature on hydrocarbon composition, 1.5:1 OP/PE, 1:1.5 OP/PS and 1:1.5 OP/PVC blends were evaluated at a range of 500-700 ºC. The experimental hydrocarbon composition obtained by varying reaction temperature are shown in Fig. 5.

Fig. 5 shows how hydrocarbon production is promoted as fast pyrolysis temperature increases. This trend varied in carbon yields depending on the feedstock selected. From the literature, higher temperatures in fast pyrolysis indicate that more energy is available for rupturing organic bonds. This could promote devolatilisation in feedstocks and facilitate endothermic co-pyrolysis reactions [16]. Regarding the1.5:1 OP/PE mass blend

364 ratio, maximum carbon yield was detected at 650 ºC, with a maximum production of
365 aliphatic compounds (93.97% of total hydrocarbons). Remarkably in Fig. 5a for 1.5:1
366 OP/PE at 650 ºC the following carbon yields were observed: 91.02% of alkenes and
367 2.94% of alkynes. Alkene yields initially accounted for 61% at 500 ºC and reached a
368 maximum value at 650 ºC. Strikingly, in the case of 1:1.5 OP/PS blend (Fig. 5b), 500 ºC
369 was selected as the optimal temperature due to the positive results obtained in aromatic
370 hydrocarbons production yields. When PS was used in the blend, aromatic carbon yields
371 declined as temperature increased, reaching minimum yields at 600 ºC. By contrast, at
372 600 ºC alkene yields reached a maximum (52.35%) for the 1:1.5 OP/PS mass blending
373 ratio. Further studies on pyrolysis established that 500-550 ºC was the optimum
374 temperature range for maximising hydrocarbon composition from waste plastic based on
375 polystyrene [5]. In Fig. 5c, carbon yields obtained from a temperature analysis of the 1:1.5
376 OP/PVC mass blending ration is shown. The results revealed a maximum yield for the
377 total sum of hydrocarbons at 650 ºC which accounted for 95.16%. Aromatics were the
378 main product detected with 64.62% of carbon yield. At lower temperatures they fell to
379 the detriment of alkenes. In contrast, when pyrolysis temperature increased, this trend
380 was reverted. This might have been due to reforming and aromatisation of alkenes, and
381 the side chains of the aromatic ring structure cracking during depolymerisation under high
382 temperature conditions [31]. In this study, no organic chloride compounds were found
383 above 500 ºC for OP/PVC blends. According to the research of Chen et al. [40],
384 interactions might occur between the pyrolysis products of PVC and the volatiles of
385 biomass pyrolysis, or between the products of PVC and the solid char residue of biomass
386 pyrolysis. To clarify this finding, ultimate and mineral content analysis were carried out
387 to the solid char residue generated by 1:1.5 OP/PVC at 650 ºC sample (Table 2). The
388 carbon content greatly increased (76.40 wt.%) while oxygen content was reduced (17.25

389 w.%) in comparison with the data from raw OP (Table 1). In addition, HSEM coupled
390 with EDX was carried out to study the residual carbon obtained after fast pyrolysis at 650
391 ºC for OP/PVC blends. As shown in Fig. 6a, the carbon residue obtained for 1:1.5
392 OP/PVC showed a porous structure. It is due to the amount of volatile matter, as well as
393 the chemical composition of OP, in which hemicellulose content was detected in higher
394 proportion (Table 1) [2,41,42]. EDX results (Fig. 6b) demonstrate that carbon, in
395 agreement with ultimate analysis (Table 2), was the major contributor to the sample.
396 Interestingly, chlorine was detected in the same weight percentage as inherent AAEMs
397 (K). Fig. 6c shows the FTIR spectrum of the obtained carbon residue. A strong absorption
398 peak at 3100-2600 cm^{-1} corresponding to the asymmetrical stretching of H-Cl was
399 observed. Moreover, an absorption peak at 750-660 cm^{-1} verified the existence of -C-Cl
400 bonds in the char residue [31]. Thus, these results suggest that the rests of chlorinated
401 compounds from PVC were retained by the char residue. It has been proposed that
402 biomass materials can act as catalyst which inhibits the dehydrochlorination process or
403 promotes the chain scission of PVC. Thus, dehydrochlorination during PVC fast pyrolysis
404 is only partly completed [43]. Similar results were obtained from Kuramochi et al. [44],
405 where chlorine emissions were reduced by the presence of wood during pyrolysis of PVC.
406 The reason suggested by these authors was that hemicellulose may reduce HCl emission
407 by fixing the Cl into the pyrolyzed residue. As commented, our results also indicates that
408 chlorinated compounds were retained in the carbon residue. Thus, it would be an effective
409 method for degradation and dechlorination of chlorine-containing plastics to produce high
410 quality liquid products. The generation of chlorinated hydrocarbons would be avoided
411 increasing the pyrolysis temperature and with the presence of inherent alkali and alkaline
412 earth metals (AAEMs) from lignocellulosic biomass, acting as adsorbents. Indeed, one

413 the typical methods to remove HCl involves the use of AAEMs as adsorbents [31, 45–
414 47].

415 Regarding the hydrocarbon distribution in the bio-oil, a significant increase in the yield
416 of aliphatic compounds for PE and aromatic hydrocarbons for PS and PVC in blend with
417 OP can be noted as reaction temperature increased. Moreover, aromatics were the main
418 products for OP with PS and PVC blends, including monocyclic aromatic hydrocarbons
419 (such as benzene, toluene and xylene) and polycyclic aromatic hydrocarbons (PAHs).
420 Both aromatics and olefins are essential as feedstock for the manufacture of valuable
421 products, such as pharmaceutical compounds, paints, solvents, among others [39].
422 Moreover, light olefins together with BTX (benzene, toluene and xylene) are the most
423 common preliminary petrochemicals [48]. To further investigate the effect of temperature
424 on the production of that valuable components, an analysis of the major fraction obtained
425 in the bio-oils were carried out. Table S1 shows a detail breakdown of the hydrocarbon
426 distribution in the bio-oils obtained at different reaction temperatures. The effect of
427 temperature on the carbon number distribution of aliphatic hydrocarbons for 1.5:1 OP/PE
428 blends is shown in Fig. 7. The aliphatic fraction was in the range of C_6-C_{20}, which were
429 mainly derived from the random chain scission of the PE [39, 48]. As temperature
430 increase, the relative content of light hydrocarbons (C_6-C_{10}) first increased and then
431 decreased, reaching the maximum at 650 ºC, accounting C_6 and C_7 maximum carbon
432 yields. On the other hand, the hydrocarbon fractions between C_{11} and C_{20} exhibited a
433 different trend, first decreasing and then increasing with reaction temperature. These
434 results suggest that the long C-C chains cracking to form light hydrocarbons (C_6-C_{10}) was
435 favoured as reaction temperature increased, being optimum at 650 ºC.

436 The influence of reaction temperature for 1:1.5 OP/PS was done focused on aromatic
437 distribution. Both PS and OP (specially lignin, one of its major chemical fractions) are

438 aromatic in nature. Additionally, there is a possibility of PAHs formation from their
439 degradation products. In this work, PAHs are categorized as naphthalene and its
440 derivatives, indene and its derivatives, and multiring aromatic components having more
441 than two rings. Fig. 8a shows the aromatic selectivity of 1:1.5 OP/PS blend as reaction
442 temperature increased. The obtained aromatic compounds were divided into benzenes
443 (benzene derivatives include ethylbenzene, propylbenzene, 2-propenylbenzene, 1-
444 propenylbenzene, cyclopropylbenzene, biphenyl, terphenyl, etc.), toluene and PAHs. The
445 presence of naphthalene and indene derivatives could be attributed to the generation of
446 methyl groups during lignin depolymerization [49]. In general, benzenes and toluene
447 selectivity decreased while PAHs were in the same percentage yield when reaction
448 temperature increased. As PAHs are undesirable in the bio-oil because they are highly
449 susceptible to coke formation [49-51], a reaction temperature of 500 ºC would be the best
450 for this blend.

451 For the 1:1.5 OP/PVC blend, the effect of temperature was studied dividing the obtained
452 aromatic fraction into benzenes and its derivatives, toluene, xylene and PAHs. For this
453 sample, it was obtained a higher yield of aromatics than the pyrolysis of the raw biomass.
454 Interestingly, the most valuable monocyclic aromatics (toluene and xylene) were found
455 for the OP/PVC blend, but not for the raw PVC. Thus, the combination of OP and PVC
456 improves the final product, generating valuable chemicals like BTX. The aromatic
457 selectivity of 1:1.5 OP/PVC blend at different reaction temperature is shown in Fig. 8b.
458 BTX were obtained in a major proportion at 650 ºC, accounting 37.9 % of aromatic
459 selectivity. Among the PAHs observed, two-ring PAH, naphthalenes and indenes,
460 dominated in all the samples. Naphthalene selectivity was decreased as reaction
461 temperature increased, from 9.7 to 6.4 %. In general, monocyclic aromatics were favoured
462 versus PAHs fractions as reaction temperature increased.

463 To sum up, the fraction of light hydrocarbons (C_6-C_{10}) was favoured as reaction
464 temperature increased for 1.5:1 OP/PE, being the optimum temperature 650 ºC. On the
465 other hand, valuable chemicals like toluene or xylene were found abundant in the bio-
466 oils, and useful aromatics like styrene or ethylbenzene were amply formed for PS and
467 PVC mixed with OP. They increased with temperature for 1:1.5 OP/PVC, but not for
468 1:1.5 OP/PS, being therefore the optimum temperature 650 ºC for the former and 500 ºC
469 for the later.

470 Pyrolytic gas was collected during fast pyrolysis experiments and analysed with FGA.
471 The fixed gas compounds that passed through the trap in fast pyrolysis at 500 ºC for the
472 materials under study are shown in Fig. 9. The thermochemical processes involved high
473 rates of temperature conducive to endothermic reactions, such as Boudouard, water-gas,
474 and steam-methane reforming [29]. The main gases given off during pyrolysis were CO,
475 CH_4, CO_2, C_2H_2, C_2H_4 and C_2H_6 and the main ones obtained throughout the whole process
476 were CO, CO_2 and CH_4 for all samples. Olive pomace had the highest CO_2 yield and CH_4
477 emissions, which correlated with the elemental analysis (Table 1). CO and CO_2 are
478 formed from thermal decomposition of oxygen functionality in their inner lignocellulosic
479 organic matrix [52]. The light hydrocarbons detected came from thermal cracking and
480 methanisation [53]. The highest CH_4 yield may have been promoted by the inherent
481 amount of potassium content in the OP sample (Table 1). This metal is reported in the
482 bibliography as an active catalyst for methanation [29]. However, there is a close
483 correlation between the H/C_{eff} ratio and pyrolytic gas emissions yields. Zhang et al. stated
484 that as the H/C_{eff} ratio feedstock rose, CO and CO_2 emissions also increased [27]. For that
485 reason, as PE is one of the polyolefins with the highest ratios of H/C_{eff}, high amounts of
486 CO and CO_2 emissions were observed. For OP, the sum of the oxygenated gases
487 represented the most important fraction detected. Furthermore, as polymers are abundant

488 sources of hydrogen, a greater amount of light hydrocarbons gases (C_2H_2, C_2H_4 and C_2H_6)
489 were detected in comparison with lignocellulosic OP. However, these gases might have
490 evolved in aromatisation, thereby enhancing carbon efficiency yields of aromatic
491 compounds in blends with OP [6].

492 Using biomass and polymers to improve fast pyrolysis product yields and quality is an
493 important issue for research on pyrolysis gas emissions. The pyrolytic gas produced from
494 the combination of biomass-polymer pyrolysis comes into contact swiftly before cooling,
495 and is catalysed into CO_2 or CO. Synergy is observed after these processes, when oxygen
496 is removed, and high-quality bio-oil is obtained [54]. Regarding the pyrolytic gas
497 emission results for the blends used, it might be concluded that they did not follow any
498 clear trend due to the synergy between the raw materials. Table 3 shows the effect of
499 temperature on yields of the gases given off which were detected for the previously
500 selected mass blending ratio samples. Overall, a reduction in CO and CO_2 product yields
501 was seen, when OP was mixed with polymers. Blends with a low H/C_{eff} ratio should
502 produce more CO by decarbonylation, as they are hydrogen-deficient compounds, which
503 probably limit the amount of oxygen transferred into water and favour CO production
504 [27]. Also, CO_2 formation by the water-gas shift reaction as a function of H/C_{eff} shows
505 the same trend as that for CO [27,55]. For the 1.5:1 OP/PE, the range of temperatures
506 between 600 to 650 ºC, limited CO_2 emission was observed. These results are coherent
507 with hydrocarbon compounds yields at those temperatures at which oxygenates were
508 suppressed. Moreover, CH_4 became the most representative gas in PE blends, due to the
509 features this plastic has, as it is a carbon chain. The effect of temperature on the 1:1.5
510 OP/PS displayed ever increasing formation of CH_4 and reached 0.55 wt.%/g-sample at
511 700 ºC. CO and CO_2 formation was largely constant throughout the range of temperature,
512 although lower gas yields were detected as temperature increased. These were in keeping

513 with the previously described trend in hydrocarbon yields. With the 1:1.5 OP/PVC
514 sample, a reduction in CO and CO_2 were observed while temperature increased.
515 Maximums oxygenate gas yields were given off in the 500-600 ºC range, where
516 hydrocarbon yields ranked low. However, PVC samples displayed similar trends for CH_4
517 with maximum yields reached as temperature increased. This was related to the decrease
518 in alkanes yields obtained.

519 In general, results indicated that CO and CO_2 formation were both reduced during co-
520 pyrolysis. While olefin and aromatic carbon yields increased for higher H/C_{eff} ratio
521 blends, CO and CO_2 carbon yields decreased. However, these outcomes implied that
522 hydrogen transfers from polymers to biomass-derived oxygenates may have mitigated
523 polymerisation and cross-linking reactions and suppressed decarbonylation and
524 decarboxylation reactions to generate CO and CO_2 [3]. According to these results, thermal
525 decomposition of CO and CO_2 fell as temperature increased. Also, light hydrocarbon
526 emissions were promoted with temperature, especially for CH_4. Thus, in conclusion, as
527 temperatures rose, thermal cracking and methanisation were promoted as the inherent
528 potassium in OP become more active as a catalyst.

529 **4. Conclusions**

530 The effects of fast pyrolysis temperature and olive pomace (OP) and agroindustrial
531 polymers (PE, PS and PVC) mass blending ratios on product distribution and
532 hydrocarbon composition were researched. Experimental results demonstrated an
533 apparent synergy with hydrocarbon yields in fast pyrolysis bio-oil at 500 ºC for the 1.5:1
534 OP/PE, 1:1.5 OP/PS and 1:1.5 OP/PVC mass ratios. Moreover, alkenes are maximised
535 for OP/PE and aromatic compounds for OP/PS and OP/PVC blends. Total hydrocarbon
536 yields increased as temperatures rose from 500 to 700 ºC. For the 1.5:1 OP/PE blend,

alkenes formation was improved, where the light hydrocarbons fraction (C_6-C_{10}) first increased and then decreased with temperature, reaching a maximum at 650 ºC. On the other hand, aromatic compounds production was enhanced for 1:1.5 OP/PS and 1:1.5 OP/PVC, with optimal temperatures at 500 and 600 ºC, respectively. The more valuable aromatic chemicals like benzenes, toluene and xylene were found to be abundantly formed for both blends. As for pyrolytic gas composition, they did not follow any trend, owing to the synergy in the blends. In general, while temperature increased, CO and CO_2 decreased and CH_4 was promoted. Finally, H_2-rich feedstocks (plastics) and a H_2-deficient (OP) offers synergy in improving aliphatic and/or aromatic carbon yields of the bio-oils formed.

CRediT authorship contribution statement

A. Alcazar-Ruiz: Conceptualization, Investigation, Writing - original draft, Data curation, Supervision. **F. Dorado**: Format analysis, Methodology, Funding acquisition, Writing - review & editing. **L. Sanchez- Silva**: Validation, Resources, Writing - review & editing.

Acknowledgements

The authors wish to thank the regional government of Castilla -La Mancha for their financial support. (Project SBPLY/17/180501/000238).

Bibliography

[1] S. Souilem, A. El-Abbassi, H. Kiai, A. Hafidi, S. Sayadi, Olive oil production sector: environmental effects and sustainability challenges, Olive Mill Waste. (2017) 1–28. doi:10.1016/B978-0-12-805314-0.00001-7.

[2] F. Dorado, P. Sanchez, A. Alcazar-Ruiz, L. Sanchez-Silva, Fast pyrolysis as an

alternative to the valorization of olive mill wastes, J. Sci. Food Agric. (2020). doi:10.1002/jsfa.10856.

[3] X. Zhang, H. Lei, S. Chen, J. Wu, Catalytic co-pyrolysis of lignocellulosic biomass with polymers: A critical review, Green Chem. 18 (2016) 4145–4169. doi:10.1039/c6gc00911e.

[4] J.N. V. Salvilla, B.I.G. Ofrasio, A.P. Rollon, F.G. Manegdeg, R.R.M. Abarca, M.D.G. de Luna, Synergistic co-pyrolysıs of polyolefin plastics with wood and agricultural wastes for biofuel production, Appl. Energy. 279 (2020) 115668. doi:10.1016/j.apenergy.2020.115668.

[5] P. Kasar, D.K. Sharma, M. Ahmaruzzaman, Thermal and catalytic decomposition of waste plastics and its co- processing with petroleum residue through pyrolysis process, J. Clean. Prod. 265 (2020) 121639. doi:10.1016/j.jclepro.2020.121639.

[6] P. Ghorbannezhad, S. Park, J.A. Onwudili, Co-pyrolysis of biomass and plastic waste over zeolite- and sodium-based catalysts for enhanced yields of hydrocarbon products, Waste Manag. 102 (2020) 909–918. doi:10.1016/j.wasman.2019.12.006.

[7] P. Europe, EPRO, Plastics - the Facts 2019, (2019). https://www.plasticseurope.org/en/resources/market-data.

[8] Cicloplast :: Reciclado de los plásticos, (n.d.). http://www.cicloplast.com/index.php?accion=notas-de-prensa&subAccion=ver-noticia&id=95&page=1&frm[keyword]=&actopc=42 (accessed January 19, 2021).

[9] M.J.B. de Souza, T.H.A. Silva, T.R.S. Ribeiro, A.O.S. da Silva, A.M.G. Pedrosa,

583 Thermal and catalytic pyrolysis of polyvinyl chloride using micro/mesoporous
584 ZSM-35/MCM-41 catalysts, J. Therm. Anal. Calorim. 140 (2020) 167–175.
585 doi:10.1007/s10973-019-08803-7.

586 [10] L. Fan, Y. Zhang, S. Liu, N. Zhou, P. Chen, Y. Cheng, M. Addy, Q. Lu, M.M.
587 Omar, Y. Liu, Bio-oil from fast pyrolysis of lignin: Effects of process and
588 upgrading parameters, Bioresour. Technol. 241 (2017) 1118–1126.

589 [11] W.N.R.W. Isahak, M.W.M. Hisham, M.A. Yarmo, T. Yun Hin, A review on bio-
590 oil production from biomass by using pyrolysis method, Renew. Sustain. Energy
591 Rev. 16 (2012) 5910–5923. doi:10.1016/J.RSER.2012.05.039.

592 [12] S. Al Arni, Comparison of slow and fast pyrolysis for converting biomass into
593 fuel, Renew. Energy. 124 (2018) 197–201. doi:10.1016/J.RENENE.2017.04.060.

594 [13] H. Stančin, M. Šafář, J. Růžičková, H. Mikulčić, H. Raclavská, X. Wang, N.
595 Duić, Co-pyrolysis and synergistic effect analysis of biomass sawdust and
596 polystyrene mixtures for production of high-quality bio-oils, Process Saf.
597 Environ. Prot. 145 (2021) 1–11. doi:10.1016/j.psep.2020.07.023.

598 [14] Q. Li, A. Faramarzi, S. Zhang, Y. Wang, X. Hu, M. Gholizadeh, Progress in
599 catalytic pyrolysis of municipal solid waste, Energy Convers. Manag. 226 (2020)
600 113525. doi:10.1016/j.enconman.2020.113525.

601 [15] A.C. Johansson, L. Sandström, O.G.W. Öhrman, H. Jilvero, Co-pyrolysis of
602 woody biomass and plastic waste in both analytical and pilot scale, J. Anal. Appl.
603 Pyrolysis. 134 (2018) 102–113. doi:10.1016/j.jaap.2018.05.015.

604 [16] B. Zhang, Z. Zhong, T. Li, Z. Xue, X. Wang, R. Ruan, Biofuel production from
605 distillers dried grains with solubles (DDGS) co-fed with waste agricultural plastic

606 mulching films via microwave-assisted catalytic fast pyrolysis using microwave
607 absorbent and hierarchical ZSM-5/MCM-41 catalyst, J. Anal. Appl. Pyrolysis.
608 130 (2018) 1–7. doi:10.1016/J.JAAP.2018.02.007.

609 [17] H. Hassan, B.H. Hameed, J.K. Lim, Co-pyrolysis of sugarcane bagasse and waste
610 high-density polyethylene: Synergistic effect and product distributions, Energy.
611 191 (2020) 116545. doi:10.1016/J.ENERGY.2019.116545.

612 [18] A. Ephraim, D.P. Minh, D. Lebonnois, C. Peregrina, P. Sharrock, A. Nzihou, A.
613 Ephraim, D.P. Minh, D. Lebonnois, C. Peregrina, P. Sharrock, Co-pyrolysis of
614 wood and plastics To cite this version : HAL Id : hal-01802140, (2018).

615 [19] Z. Li, Z. Zhong, B. Zhang, W. Wang, G.V.S. Seufitelli, F.L.P. Resende, Catalytic
616 fast co-pyrolysis of waste greenhouse plastic films and rice husk using
617 hierarchical micro-mesoporous composite molecular sieve, Waste Manag. 102
618 (2020) 561–568. doi:10.1016/j.wasman.2019.11.012.

619 [20] J. Chattopadhyay, T.S. Pathak, R. Srivastava, A.C. Singh, Catalytic co-pyrolysis
620 of paper biomass and plastic mixtures (HDPE (high density polyethylene), PP
621 (polypropylene) and PET (polyethylene terephthalate)) and product analysis,
622 Energy. 103 (2016) 513–521. doi:10.1016/j.energy.2016.03.015.

623 [21] P. Lu, Q. Huang, A.C. (Thanos) Bourtsalas, Y. Chi, J. Yan, Synergistic effects on
624 char and oil produced by the co-pyrolysis of pine wood, polyethylene and
625 polyvinyl chloride, Fuel. 230 (2018) 359–367. doi:10.1016/j.fuel.2018.05.072.

626 [22] T. Kan, V. Strezov, T.J. Evans, Lignocellulosic biomass pyrolysis: A review of
627 product properties and effects of pyrolysis parameters, Renew. Sustain. Energy
628 Rev. 57 (2016) 1126–1140. doi:10.1016/J.RSER.2015.12.185.

[23] A. Alcazar-Ruiz, R. Garcia-Carpintero, F. Dorado, L. Sanchez- Silva, Valorization of olive oil industry subproducts: ash and olive pomace fast pyrolysis, Food Bioprod. Process. 125 (2021) 37–45. doi:https://doi.org/10.1016/j.fbp.2020.10.011.

[24] TAPPI, TAPPI/ANSI Test Method T 401 om-15 - Fiber analysis of paper and paperboard, 2018.

[25] Y. Huang, S. Qiu, I.N. Oduro, X. Guo, Y. Fang, Production of High-Yield Bio-oil with a High Effective Hydrogen/Carbon Molar Ratio through Acidolysis and in Situ Hydrogenation, Energy and Fuels. 30 (2016) 9524–9531. doi:10.1021/acs.energyfuels.6b02250.

[26] Z. Wang, K.G. Burra, T. Lei, A.K. Gupta, Co-pyrolysis of waste plastic and solid biomass for synergistic production of biofuels and chemicals-A review, Prog. Energy Combust. Sci. 84 (2021) 100899. doi:10.1016/j.pecs.2020.100899.

[27] H. Zhang, Y.T. Cheng, T.P. Vispute, R. Xiao, G.W. Huber, Catalytic conversion of biomass-derived feedstocks into olefins and aromatics with ZSM-5: The hydrogen to carbon effective ratio, Energy Environ. Sci. 4 (2011) 2297–2307. doi:10.1039/c1ee01230d.

[28] O. Sanahuja-Parejo, A. Veses, M. V. Navarro, J.M. López, R. Murillo, M.S. Callén, T. García, Drop-in biofuels from the co-pyrolysis of grape seeds and polystyrene, Chem. Eng. J. 377 (2019) 120246. doi:10.1016/j.cej.2018.10.183.

[29] M. Puig-Gamero, Á. Alcazar-Ruiz, P. Sánchez, L. Sanchez-Silva, Binary Blends Versus Ternary Blends in Steam Cogasification by Means of TGA-MS: Reactivity and H<inf>2</inf>/CO Ratio, Ind. Eng. Chem. Res. 59 (2020).

652 doi:10.1021/acs.iecr.0c01399.

653 [30] F. Wu, H. Ben, Y. Yang, H. Jia, R. Wang, G. Han, Effects of different conditions
654 on co-pyrolysis behavior of corn stover and polypropylene, Polymers (Basel). 12
655 (2020). doi:10.3390/POLYM12040973.

656 [31] J. Zhou, G. Liu, S. Wang, H. Zhang, F. Xu, TG-FTIR and Py-GC/MS study of
657 the pyrolysis mechanism and composition of volatiles from flash pyrolysis of
658 PVC, J. Energy Inst. (2020). doi:10.1016/j.joei.2020.07.009.

659 [32] G. Perkins, T. Bhaskar, M. Konarova, Process development status of fast
660 pyrolysis technologies for the manufacture of renewable transport fuels from
661 biomass, Renew. Sustain. Energy Rev. 90 (2018) 292–315.
662 doi:10.1016/j.rser.2018.03.048.

663 [33] S.K. Green, R.E. Patet, N. Nikbin, C.L. Williams, C.C. Chang, J. Yu, R.J. Gorte,
664 S. Caratzoulas, W. Fan, D.G. Vlachos, P.J. Dauenhauer, Diels-Alder
665 cycloaddition of 2-methylfuran and ethylene for renewable toluene, Appl. Catal.
666 B Environ. 180 (2016) 487–496. doi:10.1016/j.apcatb.2015.06.044.

667 [34] J. Li, Y. Yu, X. Li, W. Wang, G. Yu, S. Deng, J. Huang, B. Wang, Y. Wang,
668 Maximizing carbon efficiency of petrochemical production from catalytic co-
669 pyrolysis of biomass and plastics using gallium-containing MFI zeolites, Appl.
670 Catal. B Environ. 172–173 (2015) 154–164. doi:10.1016/j.apcatb.2015.02.015.

671 [35] C. Dorado, C.A. Mullen, A.A. Boateng, Origin of carbon in aromatic and olefin
672 products derived from HZSM-5 catalyzed co-pyrolysis of cellulose and plastics
673 via isotopic labeling, Appl. Catal. B Environ. 162 (2015) 338–345.
674 doi:10.1016/j.apcatb.2014.07.006.

675 [36] F. Pinto, M. Miranda, P. Costa, Production of liquid hydrocarbons from rice crop
676 wastes mixtures by co-pyrolysis and co-hydropyrolysis, Fuel. 174 (2016) 153–
677 163. doi:10.1016/j.fuel.2016.01.075.

678 [37] A.S. Reshad, P. Tiwari, V. V. Goud, Thermal and co-pyrolysis of rubber seed
679 cake with waste polystyrene for bio-oil production, J. Anal. Appl. Pyrolysis. 139
680 (2019) 333–343. doi:10.1016/j.jaap.2019.03.010.

681 [38] Q. Van Nguyen, Y.S. Choi, S.K. Choi, Y.W. Jeong, Y.S. Kwon, Improvement of
682 bio-crude oil properties via co-pyrolysis of pine sawdust and waste polystyrene
683 foam, J. Environ. Manage. 237 (2019) 24–29.
684 doi:10.1016/j.jenvman.2019.02.039.

685 [39] M. V. Rocha, A.J. Vinuesa, L.B. Pierella, M.S. Renzini, Enhancement of bio-oil
686 obtained from co-pyrolysis of lignocellulose biomass and LDPE by using a
687 natural zeolite, Therm. Sci. Eng. Prog. 19 (2020) 100654.
688 doi:10.1016/j.tsep.2020.100654.

689 [40] Z. Chen, D. Wu, L. Chen, M. Ji, J. Zhang, Y. Du, Z. Wu, The fast co-pyrolysis
690 study of PVC and biomass for disposing of solid wastes and resource utilization
691 in N2 and CO2, Process Saf. Environ. Prot. 150 (2021) 489–496.
692 doi:10.1016/j.psep.2021.04.035.

693 [41] T.A. Lestander, L. Sandström, H. Wiinikka, O.G.W. Öhrman, M. Thyrel,
694 Characterization of fast pyrolysis bio-oil properties by near-infrared
695 spectroscopic data, J. Anal. Appl. Pyrolysis. 133 (2018) 9–15.

696 [42] S. Qiu, S. Zhang, X. Zhou, Q. Zhang, G. Qiu, M. Hu, Z. You, L. Wen, C. Bai,
697 Thermal behavior and organic functional structure of poplar-fat coal blends

during co-pyrolysis, Renew. Energy. 136 (2019) 308–316.

[43] H. Zhou, C. Wu, J.A. Onwudili, A. Meng, Y. Zhang, P.T. Williams, Effect of interactions of PVC and biomass components on the formation of polycyclic aromatic hydrocarbons (PAH) during fast co-pyrolysis, RSC Adv. 5 (2015) 11371–11377. doi:10.1039/c4ra10639c.

[44] H. Kuramochi, D. Nakajima, S. Goto, K. Sugita, W. Wu, K. Kawamoto, HCl emission during co-pyrolysis of demolition wood with a small amount of PVC film and the effect of wood constituents on HCl emission reduction, Fuel. 87 (2008) 3155–3157. doi:10.1016/j.fuel.2008.03.021.

[45] Q. Zhou, C. Tang, Y.-Z. Wang, L. Zheng, Catalytic degradation and dechlorination of PVC-containing mixed plastics via Al-Mg composite oxide catalysts, (2004). doi:10.1016/j.fuel.2004.02.015.

[46] T. Bhaskar, M.A. Uddin, J. Kaneko, T. Kusaba, T. Matsui, A. Muto, Y. Sakata, K. Murata, Liquefaction of mixed plastics containing PVC and dechlorination by calcium-based sorbent, Energy and Fuels. 17 (2003) 75–80. doi:10.1021/ef020091g.

[47] T. Karayıldırım, J. Yanık, M. Yüksel, M. Sağlam, M. Haussmann, Degradation of PVC containing mixtures in the presence of HCl fixators, J. Polym. Environ. 13 (2005) 365–374. doi:10.1007/s10924-005-5531-2.

[48] S. Krerkkaiwan, C. Fushimi, A. Tsutsumi, P. Kuchonthara, Synergetic effect during co-pyrolysis/gasification of biomass and sub-bituminous coal, Fuel Process. Technol. 115 (2013) 11–18. doi:10.1016/j.fuproc.2013.03.044.

[49] K. Praveen Kumar, S. Srinivas, Catalytic Co-pyrolysis of Biomass and Plastics

(Polypropylene and Polystyrene) Using Spent FCC Catalyst, Energy and Fuels. 34 (2020) 460–473. doi:10.1021/acs.energyfuels.9b03135.

[50] H. Zhou, C. Wu, J.A. Onwudili, A. Meng, Y. Zhang, P.T. Williams, Polycyclic Aromatic Hydrocarbon Formation from the Pyrolysis/Gasification of Lignin at Different Reaction Conditions, Energy \& Fuels. 28 (2014) 6371–6379. doi:10.1021/ef5013769.

[51] Z. Zhang, T. Hirose, S. Nishio, Y. Morioka, N. Azuma, A. Ueno, H. Ohkita, M. Okada, Chemical Recycling of Waste Polystyrene into Styrene over Solid Acids and Bases, Ind. \& Eng. Chem. Res. 34 (1995) 4514–4519. doi:10.1021/ie00039a044.

[52] M. Nasir Uddin, W.M.A.W. Daud, H.F. Abbas, Potential hydrogen and non-condensable gases production from biomass pyrolysis: Insights into the process variables, Renew. Sustain. Energy Rev. 27 (2013) 204–224. doi:10.1016/j.rser.2013.06.031.

[53] M. Widyawati, T.L. Church, N.H. Florin, A.T. Harris, Hydrogen synthesis from biomass pyrolysis with in situ carbon dioxide capture using calcium oxide, Int. J. Hydrogen Energy. 36 (2011) 4800–4813. doi:10.1016/j.ijhydene.2010.11.103.

[54] H. Chen, 4 - Lignocellulose biorefinery conversion engineering, in: H. Chen (Ed.), Lignocellul. Biorefinery Eng., Woodhead Publishing, 2015: pp. 87–124. doi:https://doi.org/10.1016/B978-0-08-100135-6.00004-1.

[55] D. López-González, M. Fernandez-Lopez, J.L. Valverde, L. Sanchez-Silva, Thermogravimetric-mass spectrometric analysis on combustion of lignocellulosic biomass, Bioresour. Technol. 143 (2013) 562–574.

doi:10.1016/J.BIORTECH.2013.06.052.

Table 1. Characteristic data analysis of the materials.

Sample	Proximate analysis (wt.%)*daf				Ultimate analysis (wt.%)*daf				HHV (MJ/kg)	H/C_{eff}
	Moisture	Ash	Volatile matter	Fixed carbon*diff	C	H	N	O*diff		
OP	1.36	3.39	79.92	15.31	49.88	6.12	0	43.99	20.01	0.15
PE	0.45	0.22	99.27	0.06	85.70	14.20	0.05	0.05	46.63	1.98
PS	0.26	2.39	97.30	0.04	92.31	7.72	0	0	41.27	1.01
PVC	0.23	1.04	98.73	0.04	40.03	5.09	0	0.65	19.87	0.09
OP Chemical composition (wt.%)*db										
	Klason Lignin				21.2					
	Hemicellulose				31.5					
	Extractives				38.1					
OP Mineral Content (wt.%)										
	Ca				0.45					
	K				3.48					
	Mg				0.068					
	Na				0.059					

*daf: dry and ash free basis; Odiff: % of oxygen calculated from difference in C, H, N and S; Fixed carbon*diff: % of fixed carbon calculated from differences in moisture, ash and volatile matter; *db: dry basis.

755 Table 2. Characteristic data analysis of 1:1.5 OP/PVC char residue at 650 ºC.

Ultimate analysis (wt.%)*daf			
C	H	N	O*diff
76.40	5.67	0.68	17.25
Mineral content (wt.%)			
Ca	K	Mg	Na
0.24	1.58	0.057	0.049

756 *daf: dry and ash free basis

757

758

759

760

761

762

763

764

765

766

767

768

769

770

Table 3. Pyrolytic gas composition results at different fast pyrolysis temperatures.

Sample	Reaction temperature (ºC)	wt.% / g-sample					
		CO	CH_4	CO_2	C_2H_2	C_2H_4	C_2H_6
1,5:1 OP/PE	500	0.17	0.21	0.26	0.16	0.13	0.09
	550	0.11	0.21	0.26	0.18	0.16	0.09
	600	0.18	0.29	0.17	0.07	0.21	0.08
	650	0.16	0.24	0.17	0.15	0.16	0.12
	700	0.15	0.10	0.26	0.23	0.12	0.13
1:1,5 OP/PS	500	0.30	0.35	0.19	0.11	0.03	0.03
	550	0.26	0.35	0.19	0.11	0.03	0.06
	600	0.07	0.31	0.36	0.14	0.04	0.09
	650	0.06	0.34	0.14	0.33	0.06	0.08
	700	0.14	0.55	0.11	0.07	0.09	0.04
1:1,5 OP/PVC	500	0.34	0.06	0.29	0.21	0.06	0.07
	550	0.32	0.09	0.29	0.17	0.06	0.07
	600	0.62	0.15	0.07	0.05	0.05	0.06
	650	0.14	0.36	0.17	0.20	0.05	0.08
	700	0.19	0.52	0.16	0.06	0.02	0.04

Figure captions

Figure 1. Schematic experimental setup of Py-GC/MS-FGA used for co-pyrolysis experiments.

Figure 2. TG and DTG profiles of OP, PE, PS and PVC; a) TGA curves and b) DTG curves for co-pyrolysis.

Figure 3. Mass ratio effect on fast pyrolysis hydrocarbon production at 500 ºC of a) OP/PE, b) OP/PS and c) OP/PVC

Figure 4. Hydrocarbon composition in the bio-oil obtained through fast pyrolysis with different H/C_{eff} ratios of a) OP/PE, b) OP/PS and c) OP/PVC feedstock blend ratios.

Figure 5. Influence of temperature fast pyrolysis on a) 1.5:1 OP/PE, b) 1:1.5 OP/PS and c) 1:1.5 OP/PVC feedstock blend ratios.

Figure 6. Characterisation analysis of the obtained 1:1.5 OP/PVC char residue after fast pyrolysis at 650 ºC: a) HRSEM image, b) EDX analysis and c) FTIR spectra.

Figure 7. Effect of reaction temperature on the carbon number distribution of aliphatic hydrocarbons in the bio-oil obtained for the 1.5:1 OP/PE sample.

Figure 8. Effect of reaction temperature on the aromatic compounds distribution in the bio-oil obtained for the a) 1:1.5 OP/PS and b) 1:1.5 OP/PVC sample.

Figure 9. Pyrolytic gas yields obtained (wt.%/g-sample) from fast pyrolysis of OP, PE, PS and PVC at 500 ºC.

Figure 1.

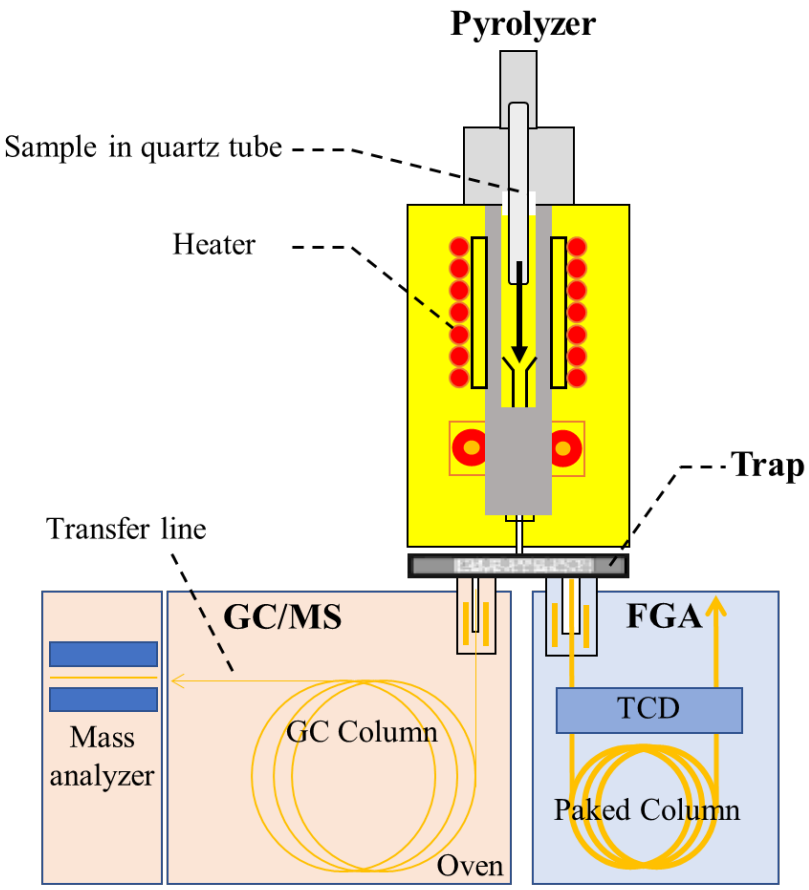
Pyrolyzer
Sample in quartz tube
Heater
Trap
Transfer line
GC/MS
FGA
Mass analyzer
GC Column
Oven
TCD
Paked Column

Figure 2.

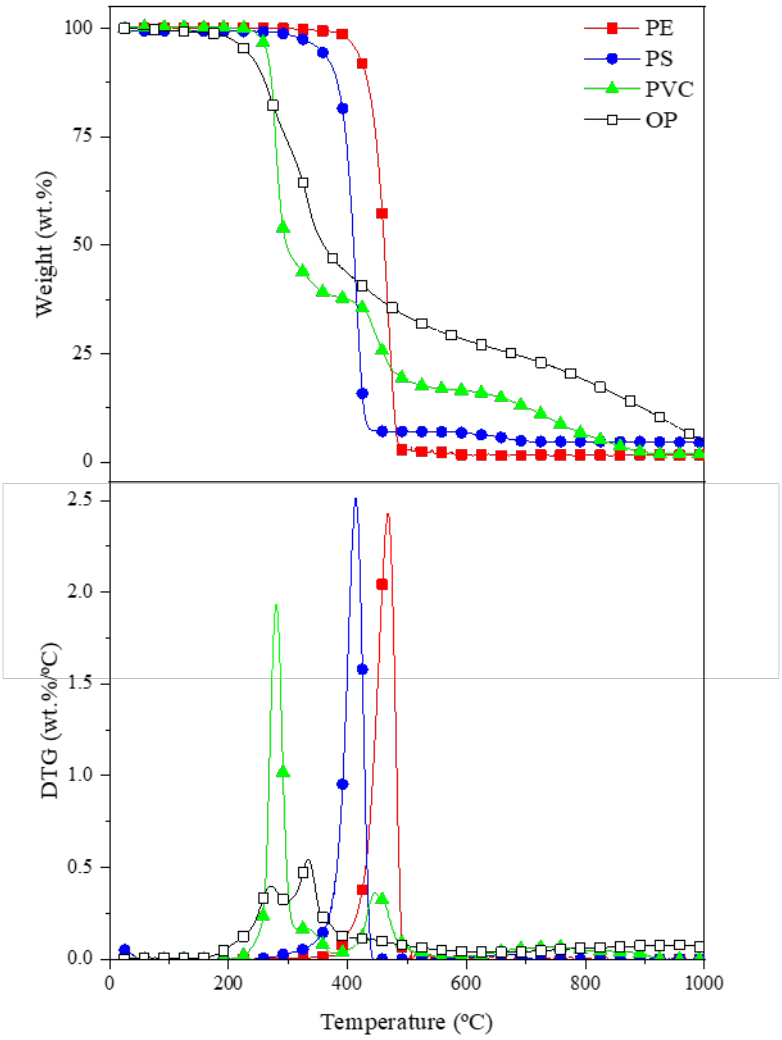
PE
PS
PVC
OP
Weight (wt.%)
100
75
50
25
0
DTG (wt.%/°C)
2.5
2.0
1.5
1.0
0.5
0.0
0
200
400
600
800
1000
Temperature (°C)

Figure 3.

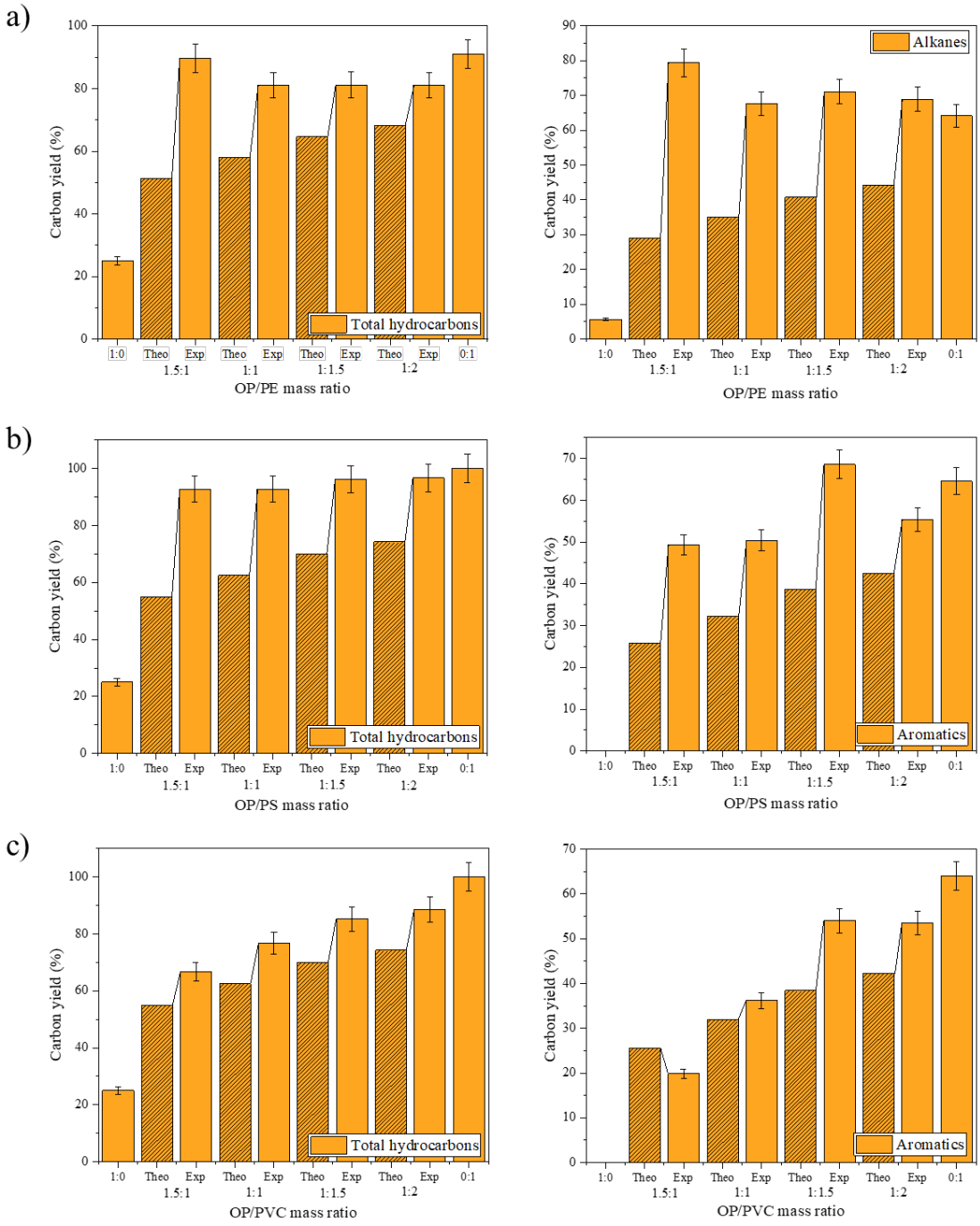
a)
Carbon yield (%)
Total hydrocarbons
Alkanes
1:0
Theo
Exp
1.5:1
1:1
1:1.5
1:2
0:1
OP/PE mass ratio
b)
Aromatics
OP/PS mass ratio
c)
OP/PVC mass ratio

Figure 4.

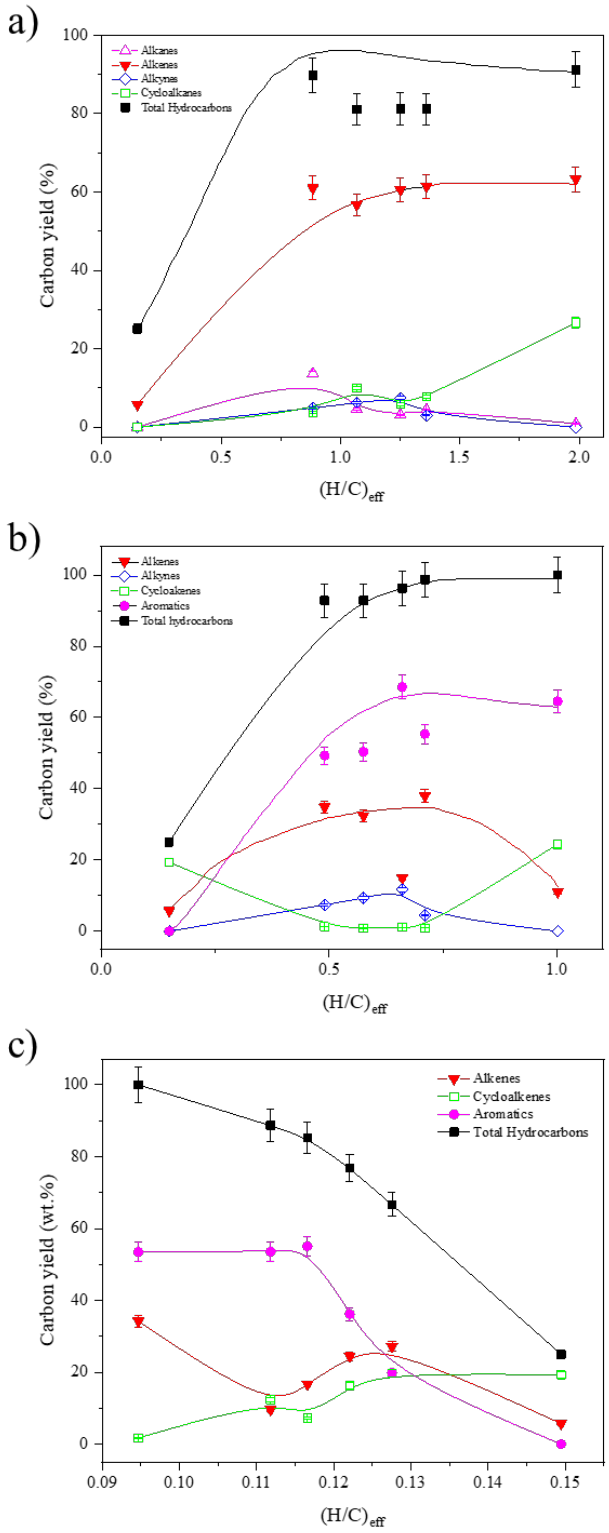
a)
Alkanes
Alkenes
Alkynes
Cycloalkanes
Total Hydrocarbons
Carbon yield (%)
(H/C)eff
b)
Alkenes
Alkynes
Cycloalkenes
Aromatics
Total hydrocarbons
Carbon yield (%)
(H/C)eff
c)
Alkenes
Cycloalkenes
Aromatics
Total Hydrocarbons
Carbon yield (wt.%)
(H/C)eff

Figure 5.

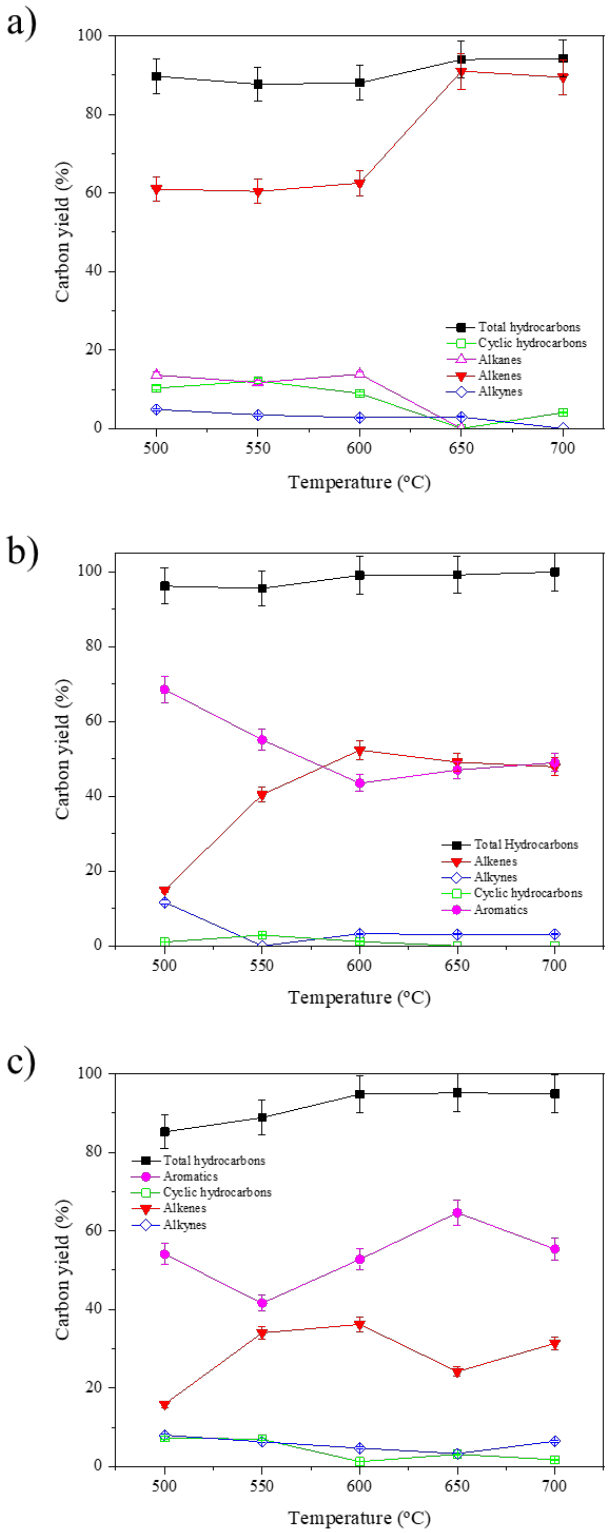
a)
Carbon yield (%)
Temperature (°C)
Total hydrocarbons
Cyclic hydrocarbons
Alkanes
Alkenes
Alkynes
b)
Carbon yield (%)
Temperature (°C)
Total Hydrocarbons
Alkenes
Alkynes
Cyclic hydrocarbons
Aromatics
c)
Carbon yield (%)
Temperature (°C)
Total hydrocarbons
Aromatics
Cyclic hydrocarbons
Alkenes
Alkynes

Figure 6.

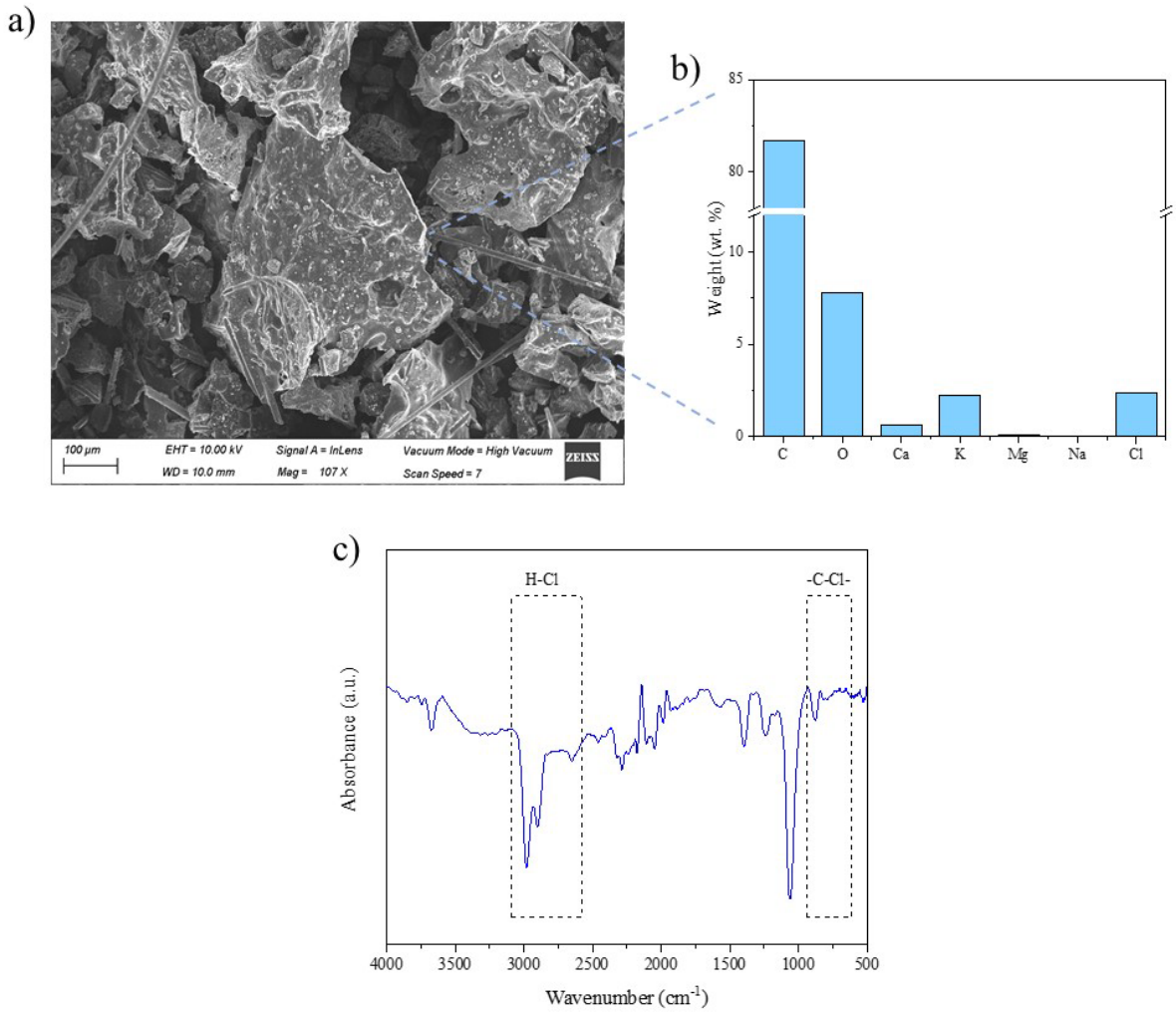
a)
100 µm
EHT = 10.00 kV
WD = 10.0 mm
Signal A = InLens
Mag = 107 X
Vacuum Mode = High Vacuum
Scan Speed = 7
ZEISS
b)
Weight (wt. %)
85
80
10
5
0
C
O
Ca
K
Mg
Na
Cl
c)
H-Cl
-C-Cl-
Absorbance (a.u.)
4000
3500
3000
2500
2000
1500
1000
500
Wavenumber (cm-1)

Figure 7.

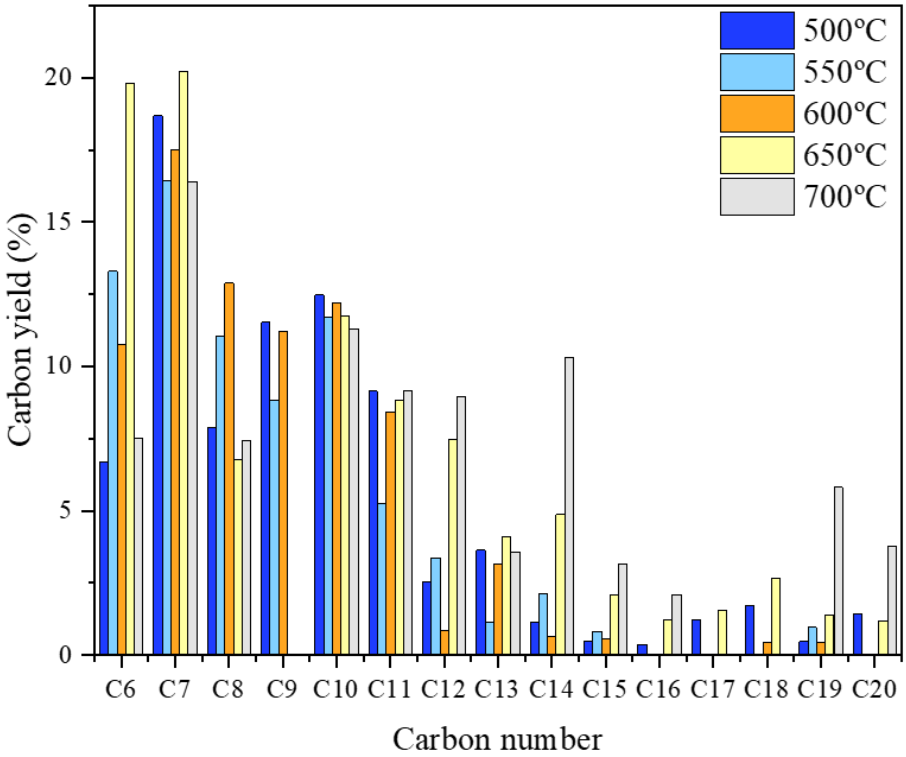
500°C
550°C
600°C
650°C
700°C
Carbon yield (%)
0
5
10
15
20
C6 C7 C8 C9 C10 C11 C12 C13 C14 C15 C16 C17 C18 C19 C20
Carbon number

878 Figure 8.

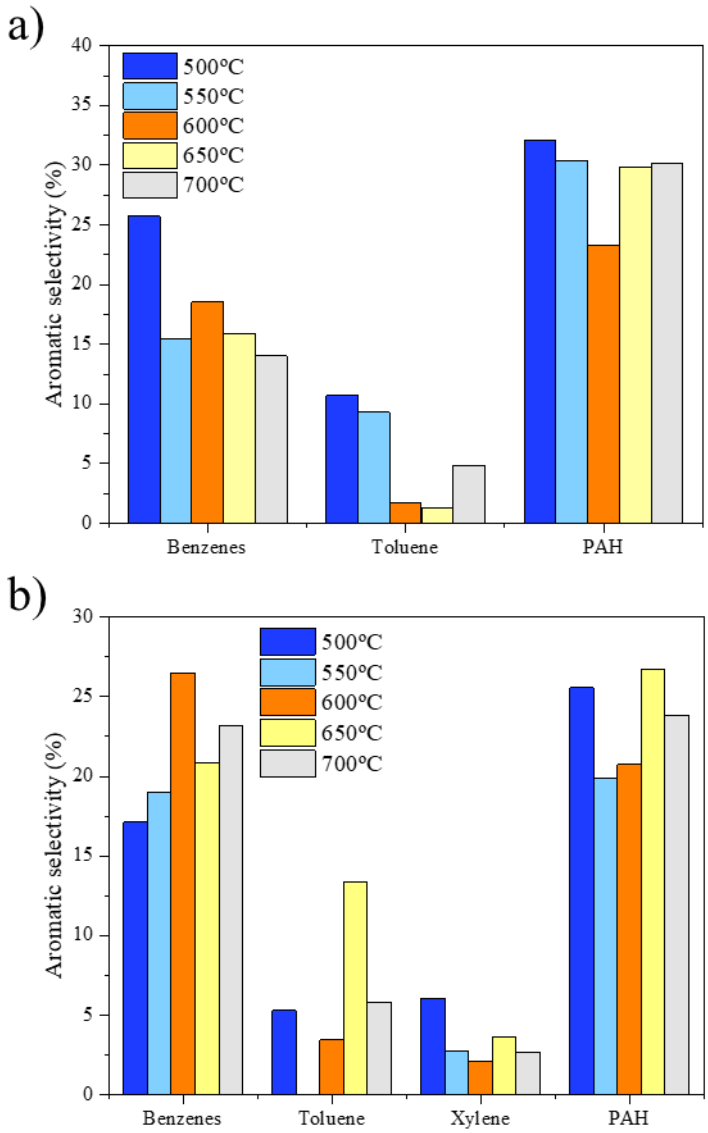

879

880

881

882

883

884

885

886

887

888

Figure 9.

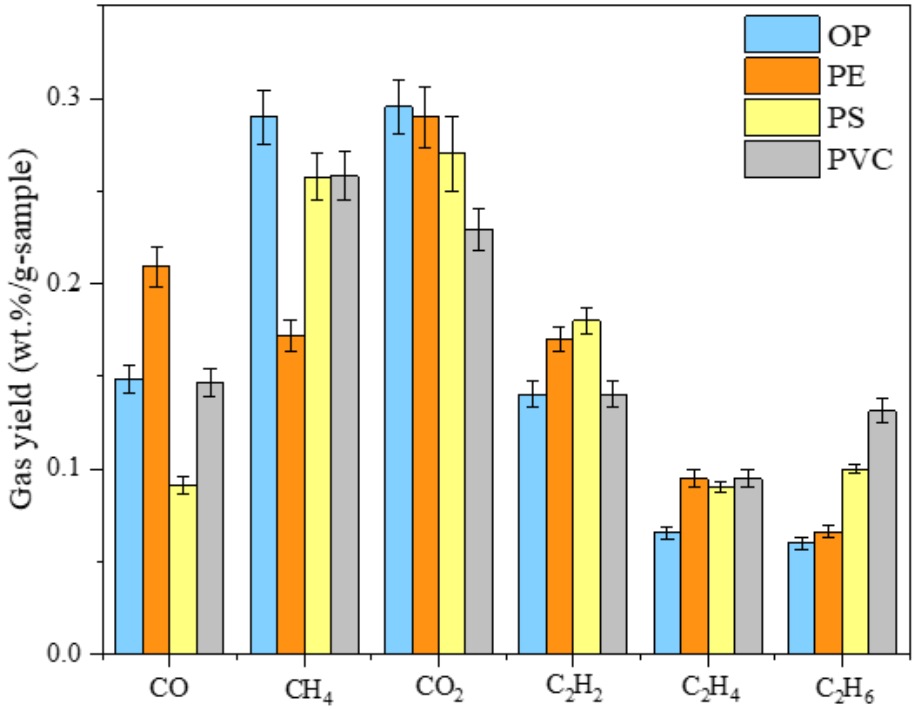
OP
PE
PS
PVC
Gas yield (wt.%/g-sample)
0.0
0.1
0.2
0.3
CO
CH_4
CO_2
C_2H_2
C_2H_4
C_2H_6